# Modulation spectroscopy at nonnormal incidence with emphasis on the vacuumuv spectral region

D. E. Aspnes, C. G. Olson, and D. W. Lynch

Citation: Journal of Applied Physics **47**, 602 (1976); doi: 10.1063/1.322620
View online: http://dx.doi.org/10.1063/1.322620
View Table of Contents: http://scitation.aip.org/content/aip/journal/jap/47/2?ver=pdfcov
Published by the AIP Publishing



# Modulation spectroscopy at non-normal incidence with emphasis on the vacuum-uv spectral region

D. E. Aspnes

*Bell Laboratories, Murray Hill, New Jersey 07974*

C. G. Olson and D. W. Lynch

*Ames Laboratory, Energy Research and Development Administration and Department of Physics, Iowa State University, Ames, Iowa 50010*

(Received 18 July 1975; in final form 8 October 1975)

Expressions are given to analyze modulation spectra taken at non-normal incidence. These expressions are used to determine the optimum angle of incidence to maximize the signal-to-noise ratio. Significant improvements are shown to be obtained in the vacuum-uv spectral region by making measurements at relatively large angles of incidence. We apply these expressions to evaluate the field-induced change in the dielectric function for the 20.5–21.0-eV core-level doublet in GaP from Schottky-barrier electroreflectance data. The line shape obtained is consistent with that of a field-modulated $M_0$ critical point modified by a Coulomb attraction between the core hole and the excited electron.

PACS numbers: 78.20.D, 78.40., 07.45.

## I. INTRODUCTION AND SUMMARY

Modulation spectroscopy at non-normal incidence[1] offers several potential advantages for analytical purposes. For $p$-polarized light, the polarization field in the substrate has components both parallel and perpendicular to the surface. This is of interest for symmetry analysis.[2–4] Substantial line-shape changes, due to the functional dependence of the Fresnel reflectance coefficients with angle of incidence $\phi$, occur upon passing through the pseudo-Brewster angle.[5] Finally, the amplification of $\Delta R/R$ as $R$ decreases near the pseudo-Brewster angle for $p$ polarization suggests that the attainable signal-to-noise ratio can be optimized by the proper choice of $\phi$.[1]

Attempts[5–11] to exploit these effects have generally been frustrated because measurements were performed in the quartz-optics range below 6 eV, where refractive indices $n$ are large for most materials. For example, if $|n|$ is large, it is not possible to develop a substantial polarization component normal to the surface for radiation propagating into the substrate for symmetry analysis purposes. Nor is it possible to obtain significant improvement of signal-to-noise ratios, which (as we shall show) requires that $|n| < 1$.

The situation is quite different in the vacuum ultraviolet (vuv), where refractive indices of substrates less than those of ambients are the rule rather than the exception. We were led to investigate these effects because we observed an approximate threefold increase in the signal-to-noise ratio in Schottky-barrier electroreflectance (ER) measurements on GaP in the 20—30-eV range, simply by changing the angle of incidence from 30° to 60°. This trivially obtainable increase in sensitivity could be understood from the Fresnel reflectivity expressions[12] and the Seraphin coefficients[13] $\alpha$ and $\beta$ evaluated at non-normal incidence. Furthermore, we needed to know the angle that the polarization field makes relative to the surface for oblique-incidence light for symmetry analysis. Our calculations proved to be useful in our current measurements[14,15] and should also be useful in future modulation-spectroscopy measurements in the vuv. Our results are not limited to ER, but rather apply to all other modulation-spectroscopy work and also to high-resolution reflectance measurements.

Our results are as follows:

(1) The Seraphin coefficients for nonnormal incidence, upon which our conclusions are based, are given in Sec. II.

(2) The sensitivity function,[16] proportional to the signal-to-noise ratio, is evaluated in Sec. III to answer the question: What angle of incidence $\phi$ should be chosen to maximize the signal-to-noise ratio? Simply stated, the answers are as follows: For $|n| \gg 1$, use $\phi = 0$ for $s$ polarization and $0 \leq \phi < \phi_B$ for $p$ polarization, where $\phi_B$ is the pseudo-Brewster angle. For $|n| < 1$, use approximately $\sin^2\phi = \mathrm{Re}(\epsilon_s/\epsilon_a)$, where $\epsilon_s$ and $\epsilon_a$ are the dielectric functions of the substrate and ambient. If $\epsilon_s$ is real, $\phi$ becomes simply the critical angle at which total internal reflection occurs.[17] For our GaP ER configuration the observed improvement in signal-to-noise in the 20—22-eV range of $\phi = 60°$ spectra relative to $\phi = 30°$ spectra for $p$ polarization was $3 \pm 1$. This was obtained by comparing average noise amplitude/peak-to-peak signal amplitude ratios of individual spectra. This value agrees well with our calculated improvement of about 3.5 for these conditions (see Fig. 3).

(3) The polarization-field angle $\theta$, relative to the surface plane, is given for GaP in Sec. IV. The *maximum* angle is given by $\tan^2\theta = |\epsilon_s|/\mathrm{Im}(\epsilon_s)$ at $\sin^2\phi = |\epsilon_s|^2/\mathrm{Re}(\epsilon_a\epsilon_s)$, if $\epsilon_s$ is such that the equation for $\phi$ has a solution.

(4) The necessary equations to calculate $\Delta\epsilon_s$, the perturbation-induced change in $\epsilon_s$, from the data and the relative reflectance change $\Delta R/R$ are given in Sec. V for any system for which the Seraphin coefficients can be calculated. We apply the results to calculate $\Delta\epsilon_{1s} = \mathrm{Re}(\Delta\epsilon_s)$ from our Schottky-barrier ER data for GaP from 20 to 22 eV. We find that the line shape of the lowest-energy structure is quite similar to that seen in ER measurements at fundamental direct edges.[18] It is

  

also quite similar to theoretical ER line shapes calculated for $M_0$ critical points with Coulomb interaction and broadening effects included.[19] This is exactly what is expected if core-level ER spectra originate from the Coulomb-modified Franz-Keldysh mechanism.

## II. SERAPHIN COEFFICIENTS AT NON-NORMAL INCIDENCE

### A. Two-phase system

Let $\epsilon_s = n_s^2$ and $\epsilon_a = n_a^2$ be the complex dielectric functions and indices of refraction that describe the substrate $s$ and ambient $a$, respectively. Then for parallel $p$ and perpendicular $s$ polarizations[12]

$$\tilde{r}_{p,as} = \frac{\epsilon_s n_{a\perp} - \epsilon_a n_{s\perp}}{\epsilon_s n_{a\perp} + \epsilon_a n_{s\perp}}, \tag{1a}$$

$$\tilde{r}_{s,as} = \frac{n_{a\perp} - n_{s\perp}}{n_{a\perp} + n_{s\perp}}, \tag{1b}$$

where

$$n_{j\perp} = (\epsilon_j - \epsilon_a \sin^2\phi)^{1/2}, \tag{2}$$

where $j = a, s$ and $\phi$ is the angle of incidence. Since $R = |\tilde{r}|^2$ we find to first order in $\Delta\epsilon_s$, a uniform perturbation-induced change in $\epsilon_s$, that[16]

$$\Delta R/R = 2\,\mathrm{Re}(\Delta\tilde{r}/\tilde{r}) \tag{3a}$$

$$= \alpha\Delta\epsilon_{1s} + \beta\Delta\epsilon_{2s} \tag{3b}$$

$$= \mathrm{Re}[(\alpha - i\beta)\Delta\epsilon_s], \tag{3c}$$

where $\alpha$ and $\beta$ are the Seraphin coefficients.[13]

For parallel and perpendicular components we find from Eqs. (1) and (3) that for the two-phase system

$$(\alpha - i\beta)_p = \frac{2n_{a\perp}(\epsilon_s - 2\epsilon_a \sin^2\phi)}{n_{s\perp}(\epsilon_s^2 \cos^2\phi - \epsilon_s\epsilon_a + \epsilon_a^2 \sin^2\phi)}, \tag{4a}$$

$$(\alpha - i\beta)_s = \frac{2n_a \cos\phi}{n_{s\perp}(\epsilon_s - \epsilon_a)}. \tag{4b}$$

### B. Three-phase systems

Let $r_{a0}$ and $r_{0s}$ represent the complex reflectances between ambient $a$ and overlayer 0, and overlayer and substrate $s$, respectively, calculated from $\epsilon_a$, $\epsilon_s$, and $\epsilon_0 = n_0^2$ by means of Eq. (1). Let

$$Z = \exp(4\pi i n_{0\perp} d/\lambda), \tag{5}$$

where $d$ is the thickness of the overlayer. It follows that

$$(\alpha - i\beta)_p = \frac{2Z\epsilon_0 n_{0\perp}(\epsilon_s - 2\epsilon_a \sin^2\phi)(1 - r_{p,a0}^2)}{n_{s\perp}(Z r_{p,a0} r_{p,0s} + 1)(Z r_{p,0s} + r_{p,a0})(\epsilon_s n_{0\perp} + \epsilon_0 n_{s\perp})^2}, \tag{6a}$$

$$(\alpha - i\beta)_s = \frac{-2Z n_{0\perp}(1 - r_{s,a0}^2)}{n_{s\perp}(Z r_{s,a0} r_{s,0s} + 1)(Z r_{s,0s} + r_{s,a0})(n_{0\perp} + n_{s\perp})^2}. \tag{6b}$$

These equations are investigated most conveniently by numerical calculations.

## III. ANGLE OF INCIDENCE TO MAXIMIZE SIGNAL

We provide here the theory for which to calculate the value of $\phi$ to maximize the signal-to-noise ratio. As Fischer and Seraphin have previously observed,[1] amplification in $\Delta R/R$ occurs for $p$ polarization as $\phi \to \phi_B$ because $R$ decreases. But it is clear that this is an oversimplified view because at the same time that $\Delta R/R$ is increasing, the reflected intensity, and therefore the over-all signal, is decreasing. For shot-noise-limited systems the appropriate measure is the sensitivity function,[16] which can be obtained by the following approach.

Let $\eta$ be the detector quantum efficiency, $\hbar\omega$ be the photon energy, and $T$ be the averaging time per data point. Then the total number of events (photoelectrons) counted during $T$ is

$$N = (\eta I_0 T/\hbar\omega)R, \tag{7}$$

where $I_0$ is the flux incident on the photodetector. The number of signal events $\Delta N$ is

$$\Delta N = \frac{\eta I_0 T}{2\hbar\omega}[(R + \Delta R) - R]$$

$$= \frac{N}{2}\frac{\Delta R}{R}, \tag{8}$$

assuming a modulation duty cycle of 0.5 (this factor is 1 in a single-beam high-resolution reflectance measurement).

Since photons follow a Poisson distribution, the shot noise $\delta N$ in an ideal system counting $N$ events is simply $\delta N = N^{1/2}$. Consequently, the signal-to-noise ratio is

$$\frac{s}{n} = \frac{\Delta N}{\delta N} \tag{9a}$$

$$= \frac{N^{1/2}}{2}\frac{\Delta R}{R} \tag{9b}$$

$$= \left(\frac{\eta I_0 T}{\hbar\omega}\right)^{1/2}\{\sqrt{R}\,\mathrm{Re}[(\alpha - i\beta)\Delta\epsilon_s]\}, \tag{9c}$$

where we have used Eq. (3c) to write Eq. (9c) in terms of $\Delta\epsilon_s$.

It is convenient to extract only that part of Eq. (9c) that depends explicitly upon the optical properties of the system. This part defines the sensitivity function

$$S = \sqrt{R}\,|\alpha - i\beta| \tag{10a}$$

$$= |\tilde{r}(\alpha - i\beta)|, \tag{10b}$$

which is independent of $\Delta\epsilon_s$ and the extrinsic parameters $\eta$, $I_0$, and $T$. Since the signal-to-noise ratio is linearly proportional to $S$, this function provides a direct measure of how a particular configuration affects the signal to noise.

The dependence of $S$ upon $\phi$ is too complicated to allow a simple general expression to be obtained giving that value of $\phi$ which maximizes $S$. But for a two-phase system, with $s$-polarized light, Eqs. (1b) and (4b) yield

$$S = \left|\frac{n_a \cos\phi}{n_{s\perp}(n_{s\perp} + n_{a\perp})^2}\right|, \tag{11}$$

where $n_{s\perp}$ and $n_{a\perp}$ are defined by Eq. (2). If $|n_s| \gg 1$, then the denominator is a slow function of $\phi$ and the maximum in $S$ occurs at $\phi = 0$. If $|n_s| < 1$, $|n_{s\perp}|$ reaches a minimum at a value that can be calculated from Eq. (2). We find that this minimum occurs at

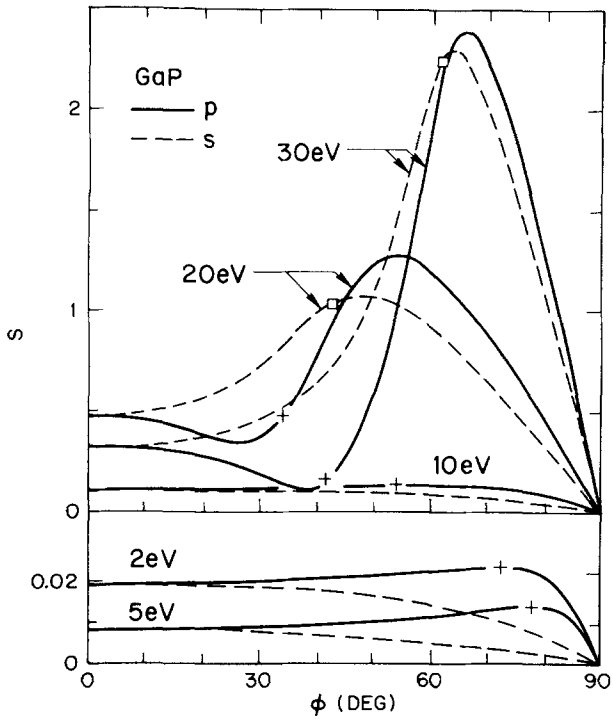


FIG. 1. Variation of the sensitivity function $S$ with angle of incidence $\phi$ for GaP for $s$ and $p$ polarization for five representative photon energies. The angles for which the reflectance for $p$ polarization is a minimum are indicated by +. The angles for which $S$ is maximum according to the approximation (12) are indicated by □. These curves were obtained using the data given in Table I.

$$\phi_{\min} \approx \sin^{-1}[\mathrm{Re}(\epsilon_s/\epsilon_a)]^{1/2}, \tag{12}$$

which provides a rough estimate of the value of $\phi$ that maximizes $S$. If $\epsilon_s$ is real, this defines the critical angle at the onset of total internal reflection.[17] Here the reflected intensity cannot be increased further and $\Delta R$, which decreases monotonically thereafter as $\phi$ increases, is as large as possible in the range of $\phi$ for which $R \approx 1$.

We have evaluated $S$ for (i) a semiconductor, GaP; (ii) a metal, Au; (iii) a semiconductor, GaP, with a 4-nm overlayer to represent a Schottky-barrier ER sample. The results for several representative photon energies are given in Figs. 1–3. Dielectric-function data for these calculations were obtained from the literature[20–25] and are given in Table I.

The results shown in Figs. 1–3 divide nicely into two categories according to whether $|n_s| > 1$ (low energies) or $|n_s| < 1$ (high energies). At low energies $S$ decreases monotonically for $s$ polarization from $\phi = 0°$ to $\phi = 90°$, whereas the maximum value of $S$ for $p$ polarization occurs very near the reflectance minimum as is expected from amplification arguments.[1]

At high energies both $s$ and $p$ polarizations show maxima at values of $\phi$ in the 60°–70° range. These values are usually well removed from the respective reflectance minima and occur at azimuth angles slightly larger than those given by the approximate expression (12). Figures 1 and 2 show particularly that values of $\phi$ near the reflectance minima are generally very poor choices

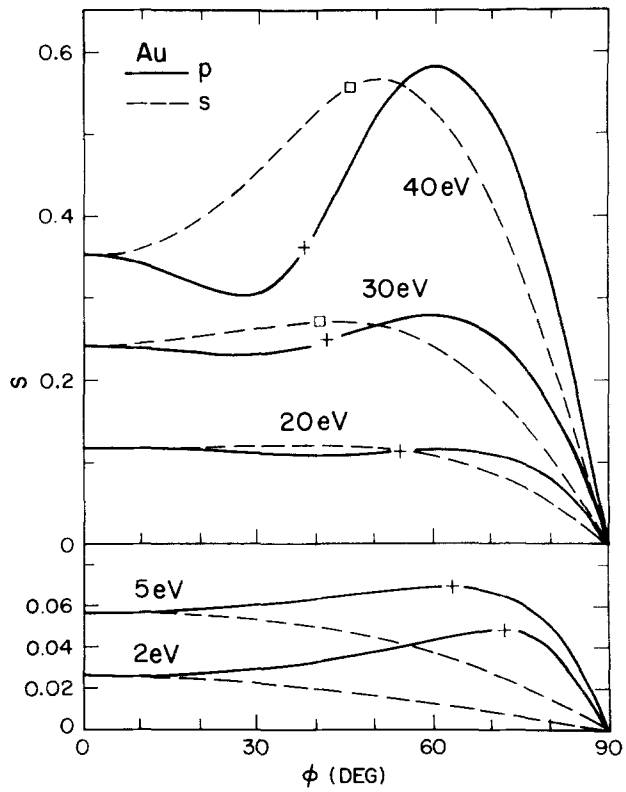


FIG. 2. As Fig. 1, but for Au.

at which to perform modulation measurements at high energies. Our observation that the signal to noise is enhanced by a factor of about $3 \pm 1$ in Ni-coated GaP in going from $\phi = 30°$ to $\phi = 60°$ is very well described by Fig. 3.

By examining Figs. 1 and 3 quantitatively, we find that a 4-nm overlayer of Ni affects $S$ much less below

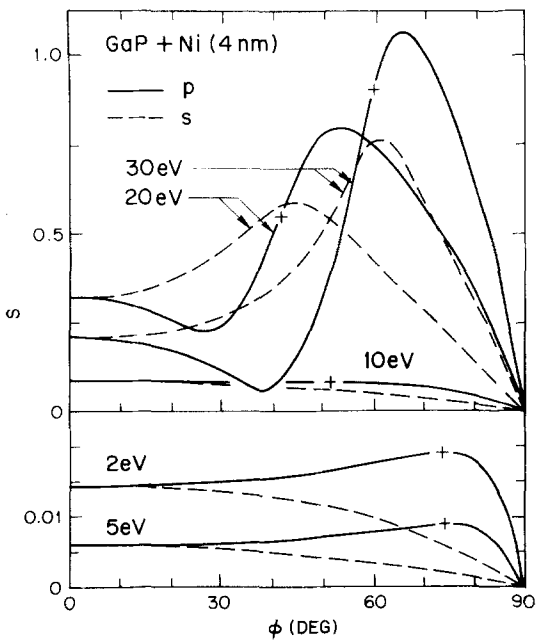


FIG. 3. As Fig. 1, but for GaP with a 4.0-nm Ni overlayer.

TABLE I. Values of dielectric functions used to calculate Figs. 1—4.

| $E$ (eV) | $\epsilon$, GaP | $\epsilon$, Au | $\epsilon$, Ni |
|---|---|---|---|
| 2 | $9.62+i0.27$ [a] | $-10.66+i1.37$ [b] | $-12.20+i16.00$ [c] |
| 5 | $2.10+i20.67$ [a] | $-0.62+i4.50$ [b] | $-2.34+i7.99$ [c] |
| 10 | $-0.50+i2.52$ [a] | $0.55+i2.85$ [d] | $0.15+i1.84$ [e] |
| 20 | $0.46+i0.26$ [f] | $1.13+i2.00$ [d] | $0.52+i0.88$ [e] |
| 30 | $0.77+i0.13$ [f] | $0.42+i1.07$ [d] | $0.8+i0.8$ [g] |
| 40 | ••• | $0.52+i0.53$ [d] | ••• |

[a] Data tabulated in R. C. Eden (Ref. 20).
[b] Johnson and Christy (Ref. 22).
[c] Johnson and Christy (Ref. 24).
[d] Hagemann *et al.* (Ref. 23).
[e] Vehse and Arakawa (Ref. 25).
[f] Calculated from $n$, $\alpha$ data of Gudat *et al.* (Ref. 21).
[g] Estimated value.

5 eV than above 20 eV. Also $s$-polarized light is affected more than $p$-polarized light. We conclude that it is not necessarily possible to determine how well a sample will work above 20 eV from measurements in the quartz-optics range. This is particularly true if an overlayer (e.g., Ni) is partially oxidized.

In internal reflection spectroscopy (IRS),[17] the physical condition $|n_a| > |n_s|$ is also encountered. We cannot apply our results directly to this case because $\Delta R/R$ in IRS has no analog in two-phase (ambient-substrate) systems. Even in three-phase systems where the overlayer is a thin film, $\Delta R/R$ must be described as a derivative with respect to film thickness rather than as a change in $\epsilon_s$. But with appropriate modifications, the sensitivity function approach[16] could also be applied to IRS.

## IV. POLARIZATION-FIELD ORIENTATION

For $p$-polarized radiation with $|n| < 1$, the component perpendicular to the surface in the substrate may be larger than that parallel to the surface. Let $\theta$ be the angle between the polarization field and the surface plane. Then

$$\tan\theta = |\mathcal{E}_z|/|\mathcal{E}_x| = n_a \sin\phi/|n_{s\perp}|, \tag{13}$$

where $n_{s\perp}$ is defined in Eq. (2).

If $|n_s| < 1$, $\theta$ can reach a maximum value at $\phi < 90°$. At maximum $\theta$, $\theta$ and $\phi$ are given by

$$\tan^2\theta = |\epsilon_s|/\mathrm{Im}(\epsilon_s), \tag{14a}$$

$$\sin^2\phi = |\epsilon_s|^2/\mathrm{Re}(\epsilon_a\epsilon_s). \tag{14b}$$

A maximum in $\theta$ will actually occur only if $0 \leq \mathrm{Re}(\epsilon_s) < 1$ and if $[\mathrm{Im}(\epsilon_s)]^2 < [\mathrm{Re}(\epsilon_s)][1-\mathrm{Re}(\epsilon_s)]$. "Transverse ER"[26] in a surface-barrier geometry is therefore rigorously possible *only* if $\mathrm{Im}(\epsilon_s) \approx 0$. Nevertheless, relatively large values of $\theta$ can be obtained in the vuv spectral region, as is indicated by the calculations for GaP shown in Fig. 4.

## V. CALCULATION OF $\Delta\epsilon_s$

Let

$$\tilde{r} = r\exp(i\theta) \tag{15}$$

be the complex reflectance of an $n$-phase plane-parallel-interface system. Then by Eqs. (3) and (15) we can write[16]

$$\Delta\epsilon_s = (\Delta r/r + i\Delta\theta)(\alpha - i\beta)^{-1}, \tag{16}$$

which expresses $\Delta\epsilon_s$ in terms of the Seraphin coefficients of the interface and where[27]

$$\frac{\Delta r}{r} = \frac{1}{2}\frac{\Delta R}{R}, \tag{17a}$$

$$\Delta\theta(\omega) = -\frac{\omega}{\pi} P\int_0^\infty \frac{d\omega'}{\omega'^2-\omega^2}\frac{\Delta R(\omega')}{R(\omega')}, \tag{17b}$$

where $\Delta R/R$ is the experimental spectrum. If $\Delta R/R$ consists of well-separated structures, then $\Delta\epsilon_s(\omega)$ can be determined from Eqs. (16) and (17) for any characterized planar system for which $\alpha$ and $\beta$ can be determined. If the field is nonuniform, then the above procedure yields an effective change $\langle\Delta\epsilon_s(\omega)\rangle$.[28]

The functional behavior of $\alpha$ and $\beta$ is too complicated to allow generalizations to be made concerning the relationship between $\Delta\epsilon_s$ and the data $\Delta R/R$, particularly in the vuv. For example, we found a strong dependence on photon energy of calculated values of $\alpha$ and $\beta$ from 16 to 30 eV for a typical Schottky-barrier ER geometry consisting of a 4-nm Ni overlayer on a GaP substrate. These variations occurred in both the amplitude $|\alpha - i\beta|$ and the relative value $\alpha/\beta$ which determine the magnitude and line shape, respectively, of $\Delta\epsilon_s$ in terms of $\Delta R/R$. Numerical evaluation of $\alpha$ and $\beta$ for specific configurations, therefore, appears to be generally necessary. By contrast, the behavior of the sensitivity function seems to be fairly simple, as shown in Figs. 1—3. It does not appear to be strongly dependent on photon energy, but shows general characteristics that depend primarily on the values of the relatively slowly varying quantities $n_a$ and $n_s$.

As an example of the use of Eqs. (4)—(6), (16), and (17), we have calculated $\Delta\epsilon_s$ from ER spectra measured for GaP over the energy range 20—22 eV. The ER data

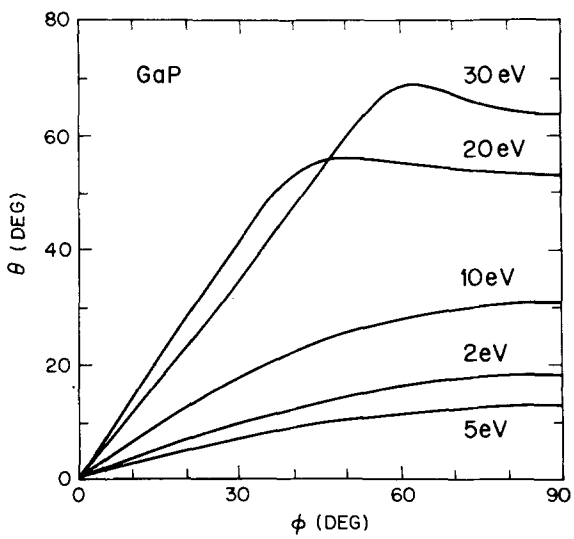


FIG. 4. Variation of the angle $\theta$ between the surface plane and the polarization field with angle of incidence for GaP for $p$ polarization for five representative photon energies.

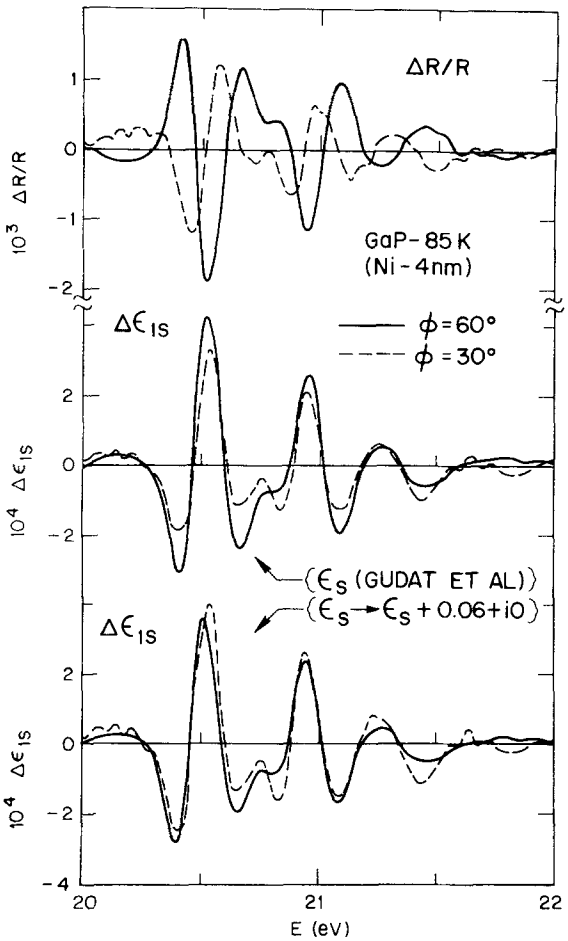


FIG. 5. (Top) Schottky-barrier ER spectra measured for an $n$-type GaP single crystal at approximately 85°K, at angles of incidence $\phi = 30°$ (dashed curve) and $\phi = 60°$ (solid curve) using predominantly $p$-polarized light. (Middle) Real component of $\Delta\epsilon_s$, the field-induced change in $\epsilon_s$, calculated for $\phi = 30°$ (dashed curve) and $\phi = 60°$ (solid curve) from the respective $\Delta R/R$ spectra at the top by means of Eqs. (3), (5), and (6), assuming a 4-nm Ni overlayer and using the $\epsilon_s$ data of Gudat *et al.* (Ref. 21). (Bottom) As in middle, except the $\epsilon_s$ data have been increased everywhere by the constant value $0.06 \pm i0.00$ for the calculations.

are shown at the top of Fig. 5 and were obtained at the Synchrotron Radiation Center of the Physical Sciences Laboratory of the University of Wisconsin by methods and equipment described previously.[14,15,29–31] Two different angles of incidence were used: $\phi = 30°$ and $\phi = 60°$. It is clear that the line shapes as well as the amplitudes of the structures in these data are quite different for the two values of $\phi$. We intentionally left the noise in these spectra to illustrate our previous points concerning the improvement of signal to noise by a factor of 3 upon increasing $\phi$ from 30° to 60°, as shown in Fig. 3.

We next used Eqs. (16) and (17) to calculate $\Delta\epsilon_s$ from these data, using the literature values for the dielectric functions of Ni [25] and GaP [21] and using a layer thickness of 4 nm for Ni. The results for $\Delta\epsilon_{1s} = \mathrm{Re}(\Delta\epsilon_s)$ are shown as the middle set of curves in Fig. 5. It is clear that the line shapes for the two angles of incidence are in much better agreement than they were for $\Delta R/R$.

However, we found that better agreement could be obtained by modifying slightly (less than 10%) the literature values for the dielectric function of GaP. This is not surprising since the coefficients $\alpha$ and $\beta$ were found to be relatively strong functions of energy (and, by inference, of $\epsilon_s$) in this spectral region.

The best agreement was obtained by adding a constant $0.06 + i0.0$ to $\epsilon_s \approx 0.5 + i0.3$ for GaP. The results for $\Delta\epsilon_{1s}$ are shown at the bottom of Fig. 5. The amplitude difference has virtually disappeared and the remaining line-shape differences are relatively minor. The adjustment of the dielectric function to obtain the best fit in $\Delta\epsilon_s$ is legitimate—if the adjustment does not exceed the experimental uncertainty in $\epsilon_s$, as is the case here.[32] We have previously pointed out[16] that the sensitivity of line shapes to configuration parameters in normal-incidence measurements on thin-film configurations where the reflectance reaches a minimum value constitutes a good argument *against* making modulation-spectroscopy measurements under these conditions. But if one is able to vary a parameter such as the angle of incidence to generate a family of curves which can be made self-consistent by small corrections in optical parameters, then the line shapes that are obtained should be reliable.

It is interesting to note that the calculated line shape of $\Delta\epsilon_{1s}$ for the lowest-energy transition at 20.50 eV in GaP is quite similar to the line shape $\Delta R/R$ for the $E_0$ transition at 0.80 eV in Ge,[18] which is itself proportional to $\Delta\epsilon_{1s}$ for that transition. Our $\Delta\epsilon_{1s}$ line shape is also in very good agreement with that calculated by Blossey[19] for the Coulomb-modified Franz-Keldysh mechanism with lifetime broading included. Although similar line shapes can be obtained by means of the low-field ER theory[33] as modified by the Slater-Koster contact exciton interaction,[34] it appears that the more accurate theoretical calculation[19] is needed to obtain a proper representation of the experimental results. A more extended analysis of this line shape for critical-point energies, broadening parameters, and symmetry effects will be given elsewhere.

## ACKNOWLEDGMENTS

The authors wish to express their appreciation to J. H. Weaver for useful discussions, to J. D. E. McIntyre for a critical reading of the manuscript, and to E. M. Rowe and the Synchrotron Radiation Center Staff where the measurements were performed. The Synchrotron Radiation Center was supported by the National Science Foundation under Grant No. DMR-74-15089.

[1] J. E. Fischer and B. O. Seraphin, Solid State Commun. 5, 973 (1967).
[2] B. O. Seraphin, in *Optical Properties of Solids*, edited by G. Haidemenakis (Gordon and Breach, New York, 1970), p. 213.
[3] N. Bottka and J. E. Fischer, Phys. Rev. B 3, 2514 (1971).
[4] V. Rehn, Surf. Sci. 37, 443 (1973).
[5] F. Lukes, cited in Ref. 1.
[6] S. Ballaro, A. Balzarotti, and V. Grasso, Phys. Status Solidi 28, K109 (1968).
[7] A. Balzarotti and M. Grandolfo, Solid State Commun. 6, 815 (1968).

[8]E. Schmidt and W.H. Knausenberger, J. Opt. Soc. Am. **59**, 857 (1969).
[9]A. Balzarotti, E. Burattini, and P. Picozzi, Phys. Rev. B **3**, 1159 (1971).
[10]V.V. Sobolev and S.N. Shestatskii, Fiz. Tver. Tela **13**, 3735 (1971) [Sov. Phys.-Solid State **13**, 3164 (1972)].
[11]K. Taniguchi, A. Moritani, C. Hamaguchi, and J. Nakai, Surf. Sci. **37**, 212 (1973).
[12]M. Born and E. Wolf, *Principles of Optics*, 5th ed. (Pergamon, New York, 1975), Sec. 1.5.
[13]B.O. Seraphin, and N. Bottka, Phys. Rev. **145**, 628 (1966).
[14]D.E. Aspnes and C.G. Olson, Phys. Rev. Lett. **33**, 1605 (1974).
[15]D.E. Aspnes, C.G. Olson, and D.W. Lynch, Phys. Rev. B **12**, 2527 (1975).
[16]D.E. Aspnes, J. Opt. Soc. Am. **63**, 1380 (1973).
[17]N.J. Harrick, *Internal Reflection Spectroscopy* (Wiley-Interscience, New York, 1967), Ch. 2.
[18]D.E. Aspnes and A. Frova, Phys. Rev. B **2**, 1037 (1970).
[19]D.F. Blossey, Phys. Rev. B **3**, 1382 (1971).
[20]R.C. Eden, thesis (Stanford University, 1967) (unpublished).
[21]W. Gudat, E.E. Koch, P.Y. Yu, M. Cardona, and C.M. Penchina, Phys. Status Solidi B **52**, 505 (1972).
[22]P.B. Johnson and R.W. Christy, Phys. Rev. B **6**, 4370 (1972).
[23]H.-J. Hagemann, W. Gudat, and C. Kunz, DESY Report No. SR-74/7, 1974 (unpublished); J. Opt. Soc. Am. **65**, 742 (1975).
[24]P.B. Johnson and R.W. Christy, Phys. Rev. B **9**, 5056 (1974).
[25]R.C. Vehse and E.T. Arakawa, Phys. Rev. **180**, 695 (1969).
[26]V. Rehn and D.S. Kyser, Phys. Rev. Lett. **18**, 848 (1967).
[27]F. Stern, in *Solid State Physics*, edited by F. Seitz and D. Turnbull (Academic, New York, 1963), Vol. 15, pp. 333ff.
[28]D.E. Aspnes and A. Frova, Solid State Commun. **7**, 155 (1969).
[29]D.E. Aspnes and A.A. Studna, Phys. Rev. B **5**, 4605 (1973).
[30]C.G. Olson, M. Piacentini, and D.W. Lynch, Phys. Rev. Lett. **33**, 644 (1974).
[31]C.G. Olson and D.W. Lynch, Phys. Rev. B **9**, 3159 (1974).
[32]W. Gudat (private communication).
[33]D.E. Aspnes, Surf. Sci. **37**, 444 (1973).
[34]J.E. Rowe and D.E. Aspnes, Phys. Rev. Lett. **25**, 162 (1970).